Eur. Phys. J. D **9**, 257–261 (1999)

THE EUROPEAN PHYSICAL JOURNAL D

EDP Sciences

Anion photoelectron spectroscopy of small boron nitride clusters: adiabatic detachment energies and vibrational frequencies of low-lying electronic states in B_2N and B_3N

K.R. Asmis, T.R. Taylor, and D.M. Neumark

Department of Chemistry, University of California, Berkeley, CA 94720, and
Chemical Sciences Division, Lawrence Berkeley National Laboratory, Berkeley, CA 94720, USA

Received: 1 September 1998 / Received in final form: 10 November 1998

Abstract. Vibrationally resolved photoelectron spectra of B_2N^- and B_3N^- at 266 nm are reported. The spectroscopy of B_3N was studied experimentally for the first time. The spectra allow us to determine adiabatic detachment energies and vibrational frequencies for several low-lying electronic states of the neutral species. Both ground state anions are shown to have linear geometries. For B_2N^- transitions to two electronic states of the neutral are observed. The electron affinity of B_2N ($\tilde{X}\,^2\Sigma_u^+$) is 3.098 ± 0.010 eV. The term energy of the electronically excited state ($\tilde{A}\,^2\Sigma_g^+$) is 0.785 eV. Transitions to three electronic states of B_3N are observed, of which the first two show vibrational structure. The adiabatic detachment energies for these two states are 2.919 eV and 3.062 eV. Preliminary calculations indicate that the photodetachment transition between the electronic ground states of B_3N^- and B_3N is spin-forbidden and therefore not observed in our spectra.

PACS. 36.40.Mr Spectroscopy and geometrical structure of clusters – 33.60.Cv Ultraviolet and vacuum ultraviolet photoelectron spectra

1 Introduction

Boron nitride clusters play an important role as precursors in the formation of ultra-hard thin solid boron nitride films, which have received considerable attention in material science [1]. Surprisingly, experimental studies on the spectroscopy of boron nitride clusters remain scarce. The diatomic BN has been studied experimentally in some detail [2–7]. B_2N, BN_2, B_2N_2 and BN_3 have been identified by matrix isolation spectroscopy combined with ab initio calculations [8–11]. No spectroscopic data is available for any of the larger boron nitride clusters. In this contribution we investigate the ground and low-lying electronic states of B_2N and B_3N.

Recent experimental studies show that B_2N is one of the most abundant species formed upon laser vaporization of solid boron nitride [8, 9, 12, 13]. Becker, Dietze, and coworkers studied the formation of boron nitride cluster anions and cations by mass spectrometry and showed that the $B_{x+1}N_x^{+/-}$ series in general and the $B_2N^{+/-}$ ions in particular are formed preferentially [12, 13]. Matrix isolation ESR spectroscopy combined with theoretical investigations suggest the lowest energy structure of B_2N to be the linear symmetric B−N−B species with a $^2\Sigma_u^+$ ground state [8]. Andrews *et al.* [9] observe two B_2N species by matrix infrared (IR) spectroscopy. Based on the observed frequencies, isotopic shifts and calculated HF/6-31G* frequencies these two species are assigned to the linear $^2\Sigma_u^+$ ground state and a low-lying, cyclic $^2B_2$ state. Ab initio calculations (QCISD(T)/6-31G*) predict two low-lying electronic states, a cyclic C_{2v} structure ($^2B_2$) and a linear $D_{\infty h}$ structure ($^2\Sigma_g^+$), at 0.069 eV and 0.740 eV, respectively, above the $^2\Sigma_u^+$ ground state [9]. Various theoretical models confirm the extraordinary thermodynamical stability of B_2N [14, 15]. The anion B_2N^- has been studied at the QCISD(T) level of theory and is predicted to have a symmetric linear structure with a $^1\Sigma_g^+$ ground state [15]. A cyclic $^3B_2$ state is calculated to lie 2.0 eV above the $^1\Sigma_g^+$ ground state.

The B_3N cation and anion have been observed in mass spectra, albeit with an order of magnitude less intensity than the corresponding B_2N ions [12, 13]. B_3N has however eluded spectroscopic characterization up to now. Several theoretical studies on its structure, energetics and harmonic vibrations are available [16–18]. The predicted lowest energy structure exhibits a linear B−B−N−B arrangement ($^1\Sigma^+$), followed by a D_{3h} structure ($^1A_1'$) 0.5 eV above the $^1\Sigma^+$ state, with C_{2v} and linear B−B−B−N configurations still higher in energy. Neither spectroscopic nor theoretical data is available on the anion B_3N^-.

We apply anion photoelectron spectroscopy of B_2N^- and B_3N^- to characterize the electronic structure of the low-lying electronic states of the corresponding neutral

species. Anion mass spectra, as well as vibrationally resolved photoelectron spectra of B_2N^- and B_3N^- are presented. The present study is a continuation of our systematic study of III-V compound clusters by anion photoelectron spectroscopy and in particular of our recent study on diatomic BN [7].

2 Experiment

The negative ion time-of-flight (TOF) photoelectron spectrometer used in this study has been described previously [19, 20]. Boron nitride clusters are generated in a pulsed molecular beam/laser ablation source, in which a rotating and translating disc of "hot-pressed" boron nitride (Carborundum Corp.) is ablated using the second harmonic of a Nd:YAG laser. The resulting plasma is entrained in a pulse of argon carrier gas and expanded through a clustering channel. Ions are extracted perpendicularly to the expansion by means of a pulsed electric field into a linear reflectron TOF mass spectrometer. At the spatial focus of the mass spectrometer, mass-selected ions are photodetached by a 266 nm laser pulse from a Nd:YAG laser. The photoelectron kinetic energy (eKE) is determined by field-free time-of-flight in a 100 cm flight tube. All photoelectron spectra presented here are plotted as a function of the electron binding energy (eBE), defined as,

$$\mathrm{eBE} = h\nu - \mathrm{eKE} \quad (1)$$

where $h\nu$ denotes the photon energy of the detachment laser. This apparatus also yields the angular distribution of the detached photoelectrons. Spectra at two laser polarizations ($\theta = 0°$ and $\theta = 90°$ with respect to the direction of the ejected electron) were recorded for both species. This allows one to distinguish overlapping transitions with different photoelectron angular distributions [7, 21]. The angular distribution can also indicate the atomic orbital parentage of the molecular orbital from which the electron is detached [22].

3 Results and discussion

3.1 Mass spectra

Two representative mass spectra of boron nitride cluster anions formed by laser ablation of a disc of "hot-pressed" boron nitride are shown in Fig. 1. The top spectrum (labeled a) was recorded at a laser fluence slightly above the threshold for the formation of significant amounts of small boron nitride clusters. Due to the natural isotope distribution of boron atoms in the sample (^{10}B 20%, ^{11}B 80%) a cluster of given stoichiometry leads to series of lines of characteristic relative intensity in the mass spectrum. The dominant species formed is B_2N^- followed by larger members of the series $B_{x+1}N_x^-$ ($B_3N_2^-$ and $B_4N_3^-$). The

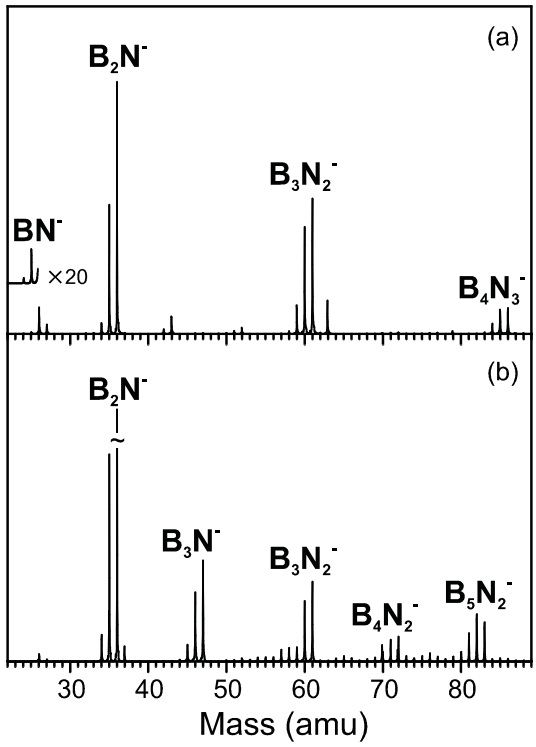

Fig. 1. Mass spectra of boron nitride cluster anions formed by laser ablation of "hot-pressed" boron nitride. The two mass spectra shown, labeled (a) and (b), were recorded under different source conditions (see text).

monomer BN^- is also observed, albeit with very low intensity. The bottom spectrum in Fig. 1 (labeled b) was recorded at 50% higher laser fluence and under source conditions optimized for the formation of boron richer clusters. The formation of the clusters B_3N^-, $B_4N_2^-$ and $B_5N_2^-$ was enhanced considerably. Throughout our studies we were not able to observe any formation of nitrogen rich clusters or of any stoichiometric clusters other than the monomer BN^-. This is in part due to the instability of clusters containing adjacent nitrogen atoms with respect to dissociation [13].

3.2 B_2N

Vibrationally resolved photoelectron spectra of B_2N^- are shown in Fig. 2. The spectra were recorded at vertical ($\theta = 0°$, top spectrum) and horizontal laser polarizations ($\theta = 90°$, bottom spectrum). We assign the observed features to photodetachment transitions from the electronic ground state of B_2N^- to two electronic states of neutral B_2N (see Table 1). The origin of the first transition (band labeled X in Fig. 1) lies at 3.098 eV. Two vibrational progressions are observed. The peak at 3.239 eV and the shoulder at 3.381 eV in the $\theta = 90°$ spectrum comprise one progression, characterized by a peak spacing of $\sim 1140\,\mathrm{cm}^{-1}$. These peaks show the same angular dependence as the origin. The second progression consists of peaks at 3.206 eV, 3.353 eV and 3.506 eV. Note that the

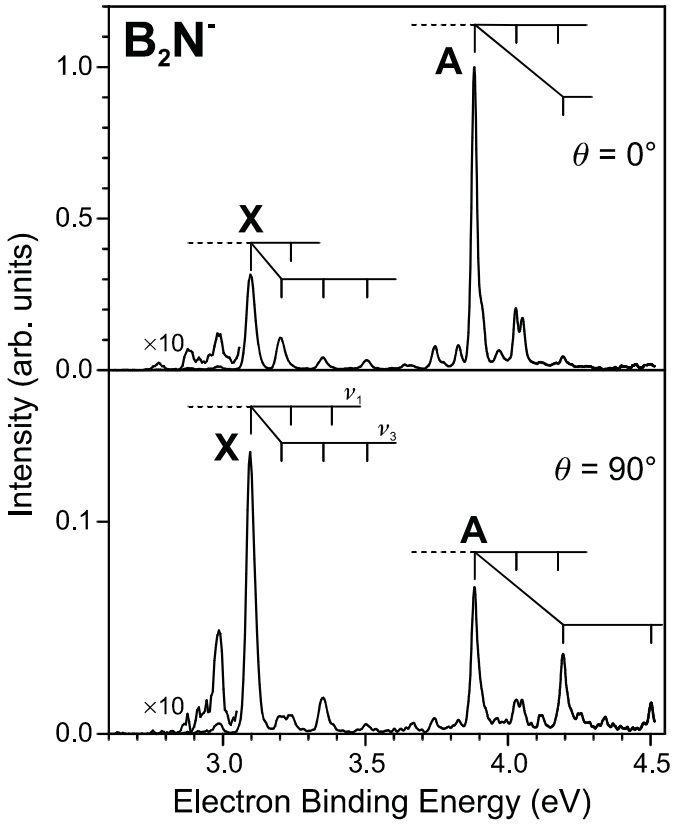

Fig. 2. Anion photoelectron spectra at 266 nm of B_2N^- measured at vertical ($\theta = 0°$) and horizontal ($\theta = 90°$) laser polarizations. The origins and vibrational progressions of the electronic ground (X) and first excited states (A) are marked. Dotted lines indicate transitions from vibrationally excited levels of the anion.

peak spacing of the second progression increases with the level of excitation and the angular dependence for each member of the progression varies. The features observed below the origin of band X are attributed to transitions originating from vibrationally excited levels of the anion electronic ground state (hot and sequence bands). The origin of the second electronic transition (band labeled A in Fig. 1) lies at 3.883 eV. The intensity of this peak is enhanced relative to the intensity of the origin of band X in the $\theta = 0°$ spectrum. The peak at 4.029 eV and the shoulder at 4.175 eV belong to one vibrational progression and the peaks at 4.193 eV and 4.502 eV to a second progression, characterized by vibrational frequencies of $\sim 1180\,\mathrm{cm}^{-1}$ and $\sim 2500\,\mathrm{cm}^{-1}$, respectively. Hot and sequence bands are again observed, in particular in the region below the origin.

We assign the two electronic transitions observed in the photoelectron spectra of B_2N^- to photodetachment to the electronic ground state ($\tilde{X}^2\Sigma_u^+$, EA = 3.098 eV) and lowest excited state ($\tilde{A}^2\Sigma_g^+$, $T_0 = 0.785$ eV) of linear B−N−B. This assignment is in agreement with previous experimental and theoretical studies. The ESR-matrix study found a $^2\Sigma_u^+$ ground state for neutral B_2N. Ab initio calculations at the QCISD(T)/6-31G* level of theory [9, 15] predict linear symmetric electronic ground states ($D_{\infty h}$ symmetry) for both B_2N^- ($\tilde{X}^1\Sigma_g^+$) and B_2N ($\tilde{X}^2\Sigma_u^+$). The first electronically excited state of linear B−N−B is calculated at 0.740 eV above the ground state. G1 theory gives a value of 3.34 eV for the electron affinity [15].

Ab initio calculations predict only a small change in the N−B bond distance for both photodetachment transitions [9, 15]. According to the Franck-Condon principle one thus expects the $\tilde{X}^2\Sigma_u^+ \leftarrow \tilde{X}^1\Sigma_g^+$ and $\tilde{A}^2\Sigma_g^+ \leftarrow \tilde{X}^1\Sigma_g^+$ transitions to result in two relatively narrow bands, each characterized by a strong $0-0$ transition and a short progression in the symmetric stretch mode (ν_1). This accounts for two of the four vibrational modes observed. We assign the $1140\,\mathrm{cm}^{-1}$ ($\tilde{X}^2\Sigma_u^+$) and $1180\,\mathrm{cm}^{-1}$ ($\tilde{A}^2\Sigma_g^+$) vibrational frequencies to the symmetric stretch mode (ν_1) in the ground and excited state, respectively, in good agreement with the scaled HF/6-31G* harmonic frequencies [23] of $1108\,\mathrm{cm}^{-1}$ and $1203\,\mathrm{cm}^{-1}$ [9]. Considering the photodetachment selection rules in combination with the predicted small change in geometry upon photodetachment, progressions in the bending (ν_2) and antisymmetric stretch (ν_3) should not be observed. Therefore it is unexpected that we observe a second progression.

We attribute the second progression for both transitions to excitation of the antisymmetric stretch vibration (ν_3). Preliminary electronic structure calculations support this assignment and indicate a strong vibronic interaction between the $\tilde{X}^2\Sigma_u^+$ and $\tilde{A}^2\Sigma_g^+$ states along the antisymmetric stretch normal coordinate. This interaction has two consequences: (1) Stabilization of the lower state and destabilization of the upper state results in considerable lowering of the "harmonic" frequency for the ν_3 mode in the ground state and raising of the frequency in the first excited state. The potential of the ν_3 mode for the ground state is actually highly non-harmonic and resembles more a square well than a harmonic potential. This explains the increase in the spacing with the level of excitation of the peaks assigned to the ν_3 mode in the $\tilde{X}^2\Sigma_u^+$ state. (2) The two electronic states are vibronically coupled, allowing forbidden transitions to borrow intensity from allowed transitions. This accounts for the irregular angular dependence of the peaks associated with the ν_3 modes. We will discuss details of these calculations in an upcoming paper. Although a cyclic B_2N species has been indicated in the previous matrix-IR study [9], no evidence for such a species is found in our photoelectron spectra or in our preliminary calculations at the CCSD(T) level of theory.

3.3 B_3N

Vibrationally resolved photoelectron spectra of B_3N^- at $\theta = 0°$ and $\theta = 90°$ are shown in Fig. 3. Our assignment of the peaks observed in the spectra is indicated in Fig. 3 and summarized in Table 1. At least three electronic transitions are observed in both spectra. The band labeled A is most intense in the $\theta = 90°$ spectrum, exhibiting an adiabatic detachment energy of 2.919 eV. A pronounced vibrational progression with a frequency of $1900\,\mathrm{cm}^{-1}$ is observed and

Table 1. Experimental adiabatic detachment energies ADE (in eV), term energies T_0 (in eV) and vibrational frequencies ν_i (in cm^{-1}) for low-lying electronic states of B_2N and B_3N.

Species	Band	ADE (eV)	T_0 (eV)	ν_i (cm^{-1})
B_2N	X ($\tilde{X}^2\Sigma_u^+$)	3.098[a]	0.000	1140 (σ_g), 870 (σ_u)[c]
	A ($\tilde{A}^2\Sigma_g^+$)	3.883	0.785	2500 (σ_u), 1180 (σ_g)
B_3N	A	2.919		1900 (σ), 750 (σ)
	B	3.062		1875 (σ), 1550 (σ), 750 (σ)
	C	4.40[b]		

[a] Electron affinity (±0.010 eV).
[b] Vertical detachment energy.
[c] First quanta of the (non-harmonic) ν_3 mode.

accounts for the three peaks observed at 3.153 eV, 3.392 eV and 3.617 eV. A second vibrational mode with a frequency of 750 cm^{-1} is also observed, although the progression in this mode is shorter. In addition, combination bands of these two vibrational modes are observed at 3.243 eV, 3.486 eV and 3.714 eV.

A second electronic state (labeled B in Fig. 3) with an origin at 3.062 eV also contributes to the signal in this region. Band B is enhanced relative to band A at $\theta = 0°$ (upper spectrum of Fig. 3). Similar to band A an extended progression is observed in a high frequency mode (1875 cm^{-1}). The first three members of this progression lie at 3.295 eV, 3.523 eV and 3.750 eV. The remaining unassigned bands below 4.2 eV can be attributed to fundamental and combination bands involving two more vibrational modes with frequencies of 1550 cm^{-1} and 750 cm^{-1}. Interestingly, the relative intensity of the combination bands involving the 1875 cm^{-1} and 1550 cm^{-1} vibrational modes increases relative to the corresponding members of the 1875 cm^{-1} progression with increasing eBE. At the moment we have no satisfactory explanation for this observation. Peaks associated with the 750 cm^{-1} mode overlap with the main progression of band A, but it is clear from the relative intensity of the peak at 3.156 eV in the $\theta = 0°$ spectrum (top spectrum in Fig. 3) that this mode contributes to the observed signal. Finally a broad, unstructured band (labeled C in Fig. 3) centered at 4.40 eV in the $\theta = 0°$ spectrum is assigned to a higher-lying excited state. This band is characterized by a sharp peak at 4.416 eV in the $\theta = 90°$ spectrum.

Previous ab initio calculations predict that the lowest potential energy structure found for B_3N exhibits a linear B−B−N−B arrangement ($C_{\infty v}$) [16–18]. The scaled MP2/6-31G* frequencies of the minimum energy $C_{\infty v}$ structure ($^1\Sigma^+$) are 1845 cm^{-1} (σ), 1044 cm^{-1} (σ), 561 cm^{-1} (σ), 231 cm^{-1} (π) and 100 cm^{-1} (π) [18]. Other possible candidates, including a D_{3h} structure and a linear B−B−B−N structure, are calculated to be considerably higher in energy and to have a highest vibrational frequency considerably lower than the observed peak spacings of 1900 cm^{-1} (band A) and 1875 cm^{-1} (band B). We therefore assign bands A and B to transitions between linear B−B−N−B species of the anion and the neutral. However, we are hesitant to assign band A to the $^1\Sigma^+$ ground state of B_3N. Our preliminary calculations at the CCSD(T) level of theory indicate that the ground state of the anion B_3N^- is not the expected $^2\Pi$ state, attained by the addition of an electron to the π^* lowest unoccupied molecular orbital of B_3N ($^1\Sigma^+$), but rather a $^4\Sigma^-$ state. In this case, the transition to the $^1\Sigma^+$ state is forbidden, because the change in total spin (ΔS) violates the one-electron transition selection rule ($\Delta S = \pm 1/2$) for photodetachment.

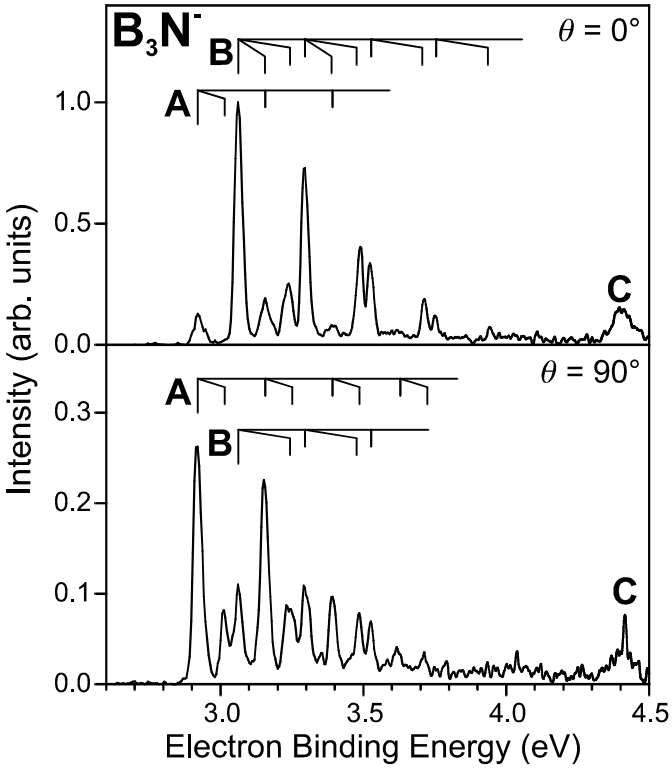

Fig. 3. Anion photoelectron spectra at 266 nm of B_3N^- measured at vertical ($\theta = 0°$) and horizontal ($\theta = 90°$) laser polarization. Origins and vibrational progressions are marked.

Additional information is needed to make a more refined assignment of the photoelectron spectra of B_2N^- and B_3N^- and to interpret the observed photoelectron angular distributions. To this end a theoretical study is currently in progress in our laboratory.

This research is supported by the National Science Foundation under Grant No. DMR-9814677. K.R. A. gratefully acknowledges a postdoctoral fellowship from the Swiss National Science Foundation.

References

1. P.B. Mirkarimi, K.F. McCarty, D.L. Medlin: Mater. Sci. Eng. R: Rep. **21**, 47 (1997)
2. A.E. Douglas, G. Herzberg: Canad. J. Res. A **18**, 179 (1940); B.A. Trush: Nature **186**, 1044 (1960)
3. O.A. Mosher, R.P. Frosch: J. Chem. Phys. **52**, 5781 (1970)
4. H. Bredohl, I. Dubois, Y. Houbrechts, P. Nzohabonayo: J. Phys. B: At. Mol. Phys. **17**, 95 (1984); H. Bredohl, I. Dubois, Y. Houbrechts, P. Nzohabonayo: J. Mol. Spec. **112**, 430 (1985); R.D. Verma: J. Phys. B **22**, 3689 (1989)
5. R.S. Ram, P.F. Bernath: J. Mol. Spec. **180**, 414 (1996)
6. M. Lorenz, J. Agreiter, A.M. Smith, V.E. Bondybey: J. Chem. Phys. **104**, 3143 (1996)
7. K.R. Asmis, T.R. Taylor, D.M. Neumark: Chem. Phys. Lett. **295**, 75 (1998)
8. L.B. Knight, D.W. Hill, T.J. Kirk, C.A. Arrington: J. Phys. Chem. **96**, 555 (1992)
9. L. Andrews, P. Hassanzadeh, T.R. Burkholder, J.M.L. Martin: J. Chem. Phys. **98**, 922 (1993)
10. C.A. Thompson, L. Andrews: J. Am. Chem. Soc. **117**, 10 125 (1995)
11. C.A. Thompson, L. Andrews, J.M.L. Martin, J. El-Yazal: J. Phys. Chem. **99**, 13 839 (1995)
12. S. Becker, H.-J. Dietze: Int. J. Mass Spectrom. Ion Processes **73**, 157 (1986)
13. G. Seifert, B. Schwab, S. Becker, D. H.-J.: Int. J. Mass Spectrom. Ion Processes **85**, 327 (1988)
14. J.M.L. Martin, J. P. François, R. Gijbels: J. Chem. Phys. **90**, 6469 (1989)
15. J.M.L. Martin, J. P. François, R. Gijbels: Chem. Phys. Lett. **193**, 243 (1992)
16. J.M.L. Martin, Z. Slanina, J.-P. François, R. Gijbels: Mol. Phys. **82**, 155 (1994)
17. Z. Slanina, J.M.L. Martin, J.-P. François, R. Gijbels: Chem. Phys. **178**, 77 (1993)
18. Z. Slanina, J.M.L. Martin, J.-P. François, R. Gijbels: Chem. Phys. Lett. **201**, 54 (1993)
19. R.B. Metz, A. Weaver, S.E. Bradforth, T.N. Kitsopoulos, D.M. Neumark: J. Phys. Chem. **94**, 1377 (1990)
20. C. Xu, G.R. Burton, T.R. Taylor, D.M. Neumark: J. Chem. Phys. **107**, 3428 (1997)
21. C. Xu, T.R. Taylor, G.R. Burton, D.M. Neumark: J. Chem. Phys. **108**, 7645 (1998)
22. K.M. Ervin, W.C. Lineberger: in *Advances in Gas Phase Ion Chemistry*, Vol. 1, ed. by N.G. Adams, L.M. Babcock (JAI Press, Greenwich, CT 1992) p. 121
23. J.A. Pople, H.B. Schlegel, R. Krishnan, D.J. DeFrees, J.S. Binkley, M.J. Frisch, R.A. Whiteside, R.F. Hout, W.J. Hehre: Int. J. Quantum Chem. Symp. **15**, 269 (1981)